Process Biochemistry 98 (2020) 160–171

Contents lists available at ScienceDirect

Process Biochemistry

journal homepage: www.elsevier.com/locate/procbio

Immobilization and characterization of horseradish peroxidase into chitosan and chitosan/PEG nanoparticles: A comparative study

Micael Nunes Melo[a,b], Fernanda Menezes Pereira[a,b], Matheus Alves Rocha[a,b], Jesica Gonçalves Ribeiro[a,b], Fernando Mendonça Diz[c], Wesley Formentin Monteiro[c], Rosane Angélica Ligabue[c], Patrícia Severino[a,b], Alini Tinoco Fricks[a,b,*]

[a] Tiradentes University, Av. Murilo Dantas 300, 49032-490, Aracaju, SE, Brazil
[b] Institute of Technology and Research, Av. Murilo Dantas 300, 49032-490, Aracaju, SE, Brazil
[c] School of Technology, Pontifical Catholic University of Rio Grande do Sul - PUCRS, Av. Ipiranga 6681, 90619-900, Porto Alegre, RS, Brazil

ARTICLE INFO

Keywords:
Horseradish peroxidase
Chitosan
Nanoparticle
Polyethylene glycol

ABSTRACT

Chitosan (CS) is considered a suitable biomaterial for enzyme immobilization. CS combination with polyethylene glycol (PEG) can improve the biocompatibility and the properties of the immobilized system. Thus, the present work investigated the effect of the PEG in the horseradish peroxidase (HRP) immobilization into chitosan nanoparticles from the morphological, physicochemical, and biochemical perspectives. CS and CS/PEG nanoparticles were obtained by ionotropic gelation and provided immobilization efficiencies (*IE*) of 65.8 % and 51.7 % and activity recovery (*AR*) of 76.4 % and 60.4 %, respectively. The particles were characterized by DLS, ZP, SEM, FTIR, TGA and DSC analysis. Chitosan nanoparticles showed size around 135 nm and increased to 229 nm after PEG addition and HRP immobilization. All particles showed positive surface charges (20 − 28 mV). Characterizations suggest nanoparticles formation and effective immobilization process. Similar values for optimum temperature and pH for immobilized HRP into both nanoparticles were found (45 °C, 7.0). V_{max} value decreased by 5.07 to 3.82 and 4.11 mM/min and K_M increased by 17.78 to 18.28 and 19.92 mM for free and immobilized HRP into chitosan and chitosan/PEG nanoparticles, respectively. Another biochemical parameters (K_{cat}, K_e, and K_α) evaluated showed a slight reduction for the immobilized enzyme in both nanoparticles compared to the free enzyme.

1. Introduction

Peroxidases (EC 1.11.1.7) are heme proteins capable to promote the oxidation of a wide range of organic and inorganic compounds by electron transferring to H_2O_2 or organic peroxides [1]. The isoenzyme C of Horseradish Peroxidase (HRP) from *Armoracia rusticana* was identified more than a century ago and is one of the most extensively characterized peroxidases. It is the most abundant and is recognized as a prototype of this class [2]. Because of its high activity and the easy detection of its oxidation products, numerous applications of HRP have been developed, such as biosensor [3], analytical and diagnostic kits [4], organic synthesis [5], decolorization of dyes [6], bioremediation of phenolic compounds [7,8] and for development of biofuel cells [9]. It is also being investigated for tissue-engineering [10] and cancer therapy [11].

Despite its wide application, HRP instability under operative conditions limits its role as a biocatalyst in industrial and commercial fields [12]. In order to overcome these inherent limitations, it is known that enzyme immobilization into solid supports may enhance industrial applications, optimizing the process performance and decreasing the overall cost [13]. Recently, there has been extensive interest in using nanoparticles (NP) for enzyme immobilization [3,7,8,14–16]. Nanoparticles enhance mobility, diffusion, thermal stability, storage capacity, expand the surface area and modulate the catalytic activity of attached enzymes [16,17].

Among the biomaterials employed in the production of nanoparticles, Chitosan (CS) has been considered as a promising carrier for enzyme immobilization due to its properties, such as abundance of functional groups, simple soluble/insoluble transition dependent on pH, resistance to chemical degradation and protection of enzyme, added to the fact that it is widely found in nature from the chitin deacetylation [18]. Furthermore, CS is a non-toxic, biodegradable, hydrophilic, antimicrobial, and chemically versatile polysaccharide, besides being cheap and to require simple ways to prepare

* Corresponding author at: Tiradentes University, Av. Murilo Dantas 300, 49032-490, Aracaju, SE, Brazil.
E-mail address: alinitf@yahoo.com.br (A.T. Fricks).

https://doi.org/10.1016/j.procbio.2020.08.007
Received 6 July 2020; Received in revised form 1 August 2020; Accepted 7 August 2020
Available online 13 August 2020
1359-5113/ © 2020 Elsevier Ltd. All rights reserved.

nanoparticles [19]. Preparation of CS nanoparticles for enzyme immobilization was reported recently in several publications [20–24].

In the search to improve the physicochemical characteristics of chitosan, polyethylene glycol (PEG) has been recognized as an effective stabilizing polymeric agent, governing size and surface charge of nanoparticles [25]. PEG may promote colloidal stability to NP based on steric repulsion due to its highly hydrophilic nature, conferring a short-range repulsive hydration layer around the particles that results in long-term stability in high salt concentrations and in a large range of pH [26]. In addition, PEG has been extensively investigated in the field of enzymatic immobilization, both as an additive during the immobilization process, which can benefit the activity of immobilized systems [27] or increase the biocompatibility of materials [28–30]. For chitosan nanoparticle this fact is important, considering that it could be a promising vector for the delivery of functional proteins in cells.

In this context and considering promising the future therapeutic applications of the immobilized enzyme, the main aim of this study is to propose HRP immobilization into CS nanoparticles (HRP-CS NP) and to investigate the effect of PEG in the formation of HRP-loaded nanoparticles (HRP-CS/PEG NP). In addition, biochemical, physicochemical, and morphological properties of the immobilized HRP samples obtained were compared.

2. Material and methods

2.1. Enzyme and reagents

Horseradish peroxidase (HRP) Type VI, RZ 3.0, EC 1.11.1.7, Chitosan (Medium Molecular Weight), Sodium Tripolyphosphate ($Na_5P_3O_{10}$, 85 %) and Polyethylene glycol (Mw = 8000 Da) (PEG8000) were purchased from Sigma-Aldrich Co. (St. Louis, USA). Guaiacol ($C_7H_8O_2$), Hydrogen Peroxide (H_2O_2, 30 %), Acetic acid ($C_2H_4O_2$), Sodium hydroxide (NaOH), Citric acid ($C_6H_8O_7$), Sodium citrate ($Na_3C_6H_5O_7$), Potassium phosphate (KH_2PO_4), Sodium bicarbonate ($NaHCO_3$) and other reagents were obtained from Vetec Ltd (Rio de Janeiro, Brazil). All solutions were prepared using distilled water.

2.2. Equipments

For the preparation of nanoparticles: Magnetic stirrer (C-MAG HS 7, IKA – Staufen, Germany), pHmeter (D-22, Digimed - São Paulo, Brazil). Determination of Particle size, polydispersity index, and zeta potential: Malvern Zetasizer Nano S (Malvern Instruments, Worcestershire, UK). Enzymatic activity: UV/Vis Spectrophotometer (Libra S22, Biochrom – Cambridge, UK), centrifuge (Rotina 380 R Benchtop, Andreas Hettich GmbH & Co. KG - Tuttlingen, Germany). For Fourier transform infrared spectroscopy (FTIR), Thermogravimetric and Differential scanning calorimetry (DSC) analyzes were used: Cary 630 Spectrophotometer (Agilent Technologies – California, USA), SDT equipment model Q600 (TA Instruments - Delaware, USA), DSC-50 cell (Shimadzu - Kyoto, Japan), respectively. For Scanning electron microscopy (SEM) was used an Inspect F50 microscope (FEI Company - Tokyo, Japan).

2.3. Preparation of CS nanoparticles, CS/PEG nanoparticles and HRP loaded nanoparticles

Nanoparticles were prepared by ionotropic gelation method adapted from Calvo et al. [31]. Briefly, chitosan (1.0 mg/mL) was dispersed in acetic acid 0.175 % (v/v) aqueous solution and maintaining by magnetic stirring for 2 h at 50 °C. The dispersion was filtered through a cellulose acetate membrane, 0.45 mm pore size, under vacuum and the pH was adjusted to 5.0 using sodium hydroxide (0.5 M). Tripolyphosphate (1.0 mg/mL) was dissolved in water using manual stirring. Nanoparticles were produced when TPP solution (28 mL) was added dropwise in the aqueous chitosan dispersion (70 mL) under magnetic stirring at room temperature for 30 min until obtaining the opalescence characteristic. CS/PEG nanoparticles were produced using the same method described, and 10.0 mg/mL PEG8000 (adapted from [32–34]) was added to CS dispersion under magnetic stirring for 30 min, followed by pH adjustment and the addition drop by drop of the TPP solution. HRP loaded nanoparticles were formed by the addition of 8.0 µg/mL of HRP to chitosan or chitosan/PEG solution under magnetic stirring for 30 min at 25 °C before the incorporation of TPP solution. The samples were stored at 4 °C in their natural form or lyophilized to obtain solid particles.

2.4. Particle size, polydispersity index and zeta potential

Mean size and polydispersity index (PDI) of the nanoparticles were determined by Dynamic Light Scattering (DLS) technique. 1 mL of nanoparticle solutions was added in polystyrene cuvettes and the analysis was carried out at a scattering angle of 90° at room temperature. The surface charge of the nanoparticles was measured by Zeta Potential (ZP). Samples were loaded into a capillary cell and analyzed at 25 °C. The results were reported as an average value of triplicate (n = 3).

2.5. Enzyme activity assay

Enzymatic activity of HRP was measured as formation of tetraguaiacol ($\varepsilon_{tetraguaiacol} = 26.6\ mM^{-1}\ cm^{-1}$ [35]) by oxidation of guaiacol at 25 °C in the presence of H_2O_2 according to literature [1,5]. The reaction was monitored at 470 nm. The HRP assay medium contains 2.76 mL of phosphate buffer (100 mM, pH 6.0), 0.04 mL of HRP (1.6 µg/mL), 0.1 mL of guaiacol (100 mM), and 0.1 mL of H_2O_2 (2.0 mM). For the measurement of HRP loaded nanoparticles proportional amounts of enzyme were calculated to use an equivalent volume on the reaction. One enzyme unit (U) was defined as the amount of enzyme capable to produce 1 µmol of product in 1 min at specific temperature and pH for this reaction.

2.6. Determination of activity recovery (AR) and immobilization efficiency (IE)

Nanoparticles obtained were centrifugated at 10,000 x *g*, 4 °C for 1 h. *AR* and *IE* was determined conform Eq. 1 and Eq. 2:

$$AR\ (\%) = U_s / U_o \times 100 \quad (1)$$

$$IE\ (\%) = U_o - U_f / U_o \times 100 \quad (2)$$

Where U_s is total units enzymatic activity present in the medium, U_o is units of peroxidase activity offered for immobilization and *Uf* is free units of peroxidase presents in the supernatant after centrifugation.

2.7. FTIR

Samples were performed by FTIR on equipment with a zinc selenide crystal (ZnSe) and an ATR (total attenuated reflection) device. About 2 mg of the lyophilized samples were deposited on the crystal surface in a spectral range of 650 - 4000 cm^{-1} under resolution of 2 cm^{-1} and processed for automatic data acquisition using the Agilent MicroLab PC software.

2.8. Thermal analysis

Thermogravimetric analysis (TGA) was performed using 5.0 mg of the samples supported in a alumina crucible, using a flow rate of 10 mL/min and heating rate of 10 °C/min, from 35 °C to 500 °C under nitrogen atmosphere. DSC was performed under a dynamic nitrogen atmosphere with a flow rate of 50 mL/min and heating rate of 10 °C/min from 35 to 500 °C. The samples were analyzed in closed aluminum capsules with a sample mass of 2.0 mg.

2.9. SEM

Morphological properties of the nanoparticles before and after HRP immobilization were evaluated by a Field-Emitting Scanning Electron Microscopy (SEM-FEG). Liquid samples were added to the stumps covered with carbon tape, dried at 40 °C for 2 h, and then metallized in the secondary electron mode (gold metallization).

2.10. Effect of temperature and pH on enzyme activity

The effect of temperature on free and immobilized HRP was tested by performing the activity in the various temperatures ranging from 25 to 65 °C. The highest value of enzyme activity in each set was assigned as 100 % activity. The effect of pH on free and immobilized HRP activity was carried out at different pH values ranging from 4.0–9.0 using 0.1 M citric acid-sodium citrate (pH 4.0–5.0), 0.1 M potassium phosphate (pH 6.0–8.0), and 1 M sodium bicarbonate-carbonate (pH 9.0). The result was expressed in form of relative activity, using the same criteria as the optimum temperature.

2.11. Determination of kinetic parameters

Kinetic parameters of the free and immobilized HRP were determined conform the topic 2.5 by measuring the rates of the reaction at various guaiacol concentrations ranging from 10 to 100 mM. The kinetic parameters K_M, V_{max} were calculated from the Lineweaver–Burk plot, and their derivative constants (catalytic constant - K_{cat}, specific constant - K_e and diffusion constant - K_α) were determined conform Eq. 3, Eq 4 and Eq.5.

$$K_{cat} = V_{max} / [E]_0 \quad (3)$$

$$K_\alpha = V_{max} / K_M \quad (4)$$

$$K_e = K_{cat} / K_M \quad (5)$$

Where $[E]_0$ corresponds to the initial concentration of enzyme offered in the reaction.

2.12. Statistical analysis

All the experiments were realized in triplicate and the experimental results were expressed as standard error of the mean (mean ± S.E.) or represented as error bars in figures, and were analyzed for statistical significance by one-way and two-way analysis of variance (ANOVA) followed by Tukey or Bonferroni post-test, respectively (*** $p < 0.001$; ** $p < 0.01$; * $p < 0.05$) (Prims GraphPAD® 7.0).

3. Results and discussion

3.1. Particle size, polydispersity index and zeta potential of nanoparticles

Nanoparticles were produced by the ionotropic gelation method using CS:TPP ratio of 5:2 (w/w). Chitosan dispersed in an aqueous acid medium (pH 5.0) shows a protonated amino group (NH_3^+) that interacts electrostatically with a negative charge ($P_3O_{10}^{5-}$ and $HP_3O_{10}^{4-}$) from sodium tripolyphosphate. This method results in the spontaneous formation of positively charged NP without the use of organic solvent or surfactant [36]. Also, the crosslinking between the PEG hydroxyl groups (OH) and the protonated amino groups (NH_3^+) of chitosan was responsible for the formation of a CS/PEG network before the gelation process [32].

Nanoparticles were evaluated for the mean diameter (nm), polydispersity index (PDI) and zeta potential (ZP), and the values obtained are presented in Table 1. For all CS nanoparticles the PDI was less than 0.5 thus indicating a narrow and favorable particle size distribution. Guidelines classifying NP-dispersions with ZP values of ± 20 − 30 mV as moderately stable [37]. The ZP values of the nanostructured systems in the present study indicate stability (ZP values between +20.1 and +28.4 mV). CS NP showed a mean size of 134.7 ± 1.9 nm, 0.24 ± 0.03 of polydispersity index (PDI) and 24.4 ± 0.8 mV of zeta potential. Similar results are obtained by [32,38] that prepare CS NP in similar conditions. Also, the positive surface charge occurs due to the presence of protonated amino groups of chitosan in the marginal region of the particle [39].

PEG addition increased the mean size of nanoparticles ~ 40 nm (171 ± 5.0 nm) and the polydispersity index increases to 0.35 ± 0.04. Otherside, the surface charge reduced to 20.1 ± 0.4 mV. All changes mentioned were statistically significant ($p < 0.001$). The increase in size and reduction in zeta potential suggests the production of the PEG-crosslinked chitosan nanoparticles [32,40]. These changes probably occurred due to the large volume of the PEG flexible chains interacting their electronegative oxygen atoms through hydrogen bonds with the free electropositive aminic hydrogens of chitosan, especially on the outside of the nanoparticles. This interaction forms a semi-interpenetrating network, which is characterized by the physical combination of two network polymers in the absence of covalent bonds, where one of the polymers is crosslinked and the other is linear [31,40].

The predilection for the surface of the particle has its behavior justified because the voluminous PEG hydrophilic molecule tends to move to the surface of the nanoparticles in order to maintain contact with the aqueous medium, resulting in a decrease of zeta potential [39]. It has been shown that high molecular weight PEG, notably PEG 8000, has a greater ability to stabilize nanoparticles by steric repulsion compared to lower molecular weight PEG [34].

After HRP immobilization, the mean size of HRP-CS NP ranged to 169.8 ± 9.6 nm and PDI increased to 0.41 ± 0.03, indicating a relatively homogeneous dispersion [41]. In addition, zeta potential increased to +28.4 ± 1.1 mV. Similarly to the occurred after the incorporation of PEG, changes in the average diameter, surface charge and PDI of the particles showed statistical significance ($p < 0.001$) when compared to the CS NP before the addition of HRP.

The mean diameter of the HRP-CS/PEG NP increased to 229.0 ± 13.0 nm, and PDI increasing to 0.45 ± 0.02. Similarly, zeta potential increased to +25.9 ± 0.7 mV. The reasons for these changes are the same as those already discussed for HRP-CS NP. The increase in the mean diameter of the HRP-CS/PEG NP higher than all other analyzed particles suggests both the PEG crosslinking and the enzyme encapsulation into the nanoparticle, representing a statistical significance when compared to both CS/PEG NP ($p < 0.001$ to size and ZP) and HRP-CS NP ($p < 0.001$ to size and $p < 0.01$ to ZP).

In the present work, all the HRP-loaded nanoparticles are larger than empty nanoparticles, possibly due to the high molecular mass (44 KDa) and the diameter of the HRP molecules (between 6 and 8 nm) [42,43]. Changes in the size of nanomaterials are a strong indication of the presence of enzymes incorporated into the structure of these supports. In a study carried out by Rodríguez-Deluna et al. [44], the average diameter of polyvinyl alcohol nanofibers increased from 118 nm in the absence of HRP to 186 nm from the addition of 6 μg of HRP/g of nanofiber. The authors attributed the increase in the nanofiber diameter distribution to the fact that the enzyme increases the molecular weight in the polymer solution, resulting in the size modification of the nanofibers [44].

On the other hand, the presence of HRP increased the zeta potential of the nanoparticles. Oliver et al. [45], using the isoelectric focusing gel technique, determined that the type VI HRP (isoenzyme also used in this work), has a basic pI of 8.3, which would give a positive charge to most of the HRP molecules in pH 5.0. This enzyme characteristic reinforces the most positive ZP of the CS-HRP NP and HRP-CS/PEG NP when compared to the CS NP and CS/PEG NP, respectively.

Table 1
Summary of mean size, polydispersity index (PDI), zeta potential (ZP), and enzyme content values (Activity recovey – *AR* and Immobilization Efficiency – *IE*) for Chitosan nanoparticles (CS NP), HRP-loaded chitosan nanoparticles (HRP-CS NP), Chitosan/Polyethylene glycol nanoparticles (CS/PEG NP), and HRP-loaded Chitosan/Polyethylene glycol nanoparticles (HRP-CS/PEG NP).

Sample	Size (nm)	PDI	ZP (mV)	*AR* (%)	*IE* (%)
CS NP	134.7 ± 1.9	0.24 ± 0.03	24.4 ± 0.8	–	–
HRP-CS NP	169.8 ± 9.6	0.41 ± 0.03	28.4 ± 1.1	76.4 ± 4.2	65.8 ± 0.5
CS/PEG NP	171.7 ± 5.0	0.35 ± 0.04	20.1 ± 0.4	–	–
HRP-CS/PEG NP	229.0 ± 13.0	0.45 ± 0.02	25.9 ± 0.7	60.4 ± 6.9	51.7 ± 1.7

3.2. Immobilization of HRP into CS and CS/PEG nanoparticles

CS NP showed higher *AR* and *IE* results compared to CS/PEG NP. *AR* of encapsulated HRP in chitosan nanoparticles was 76.4 %, while HRP encapsulated into CS/PEG nanoparticles present an *AR* of 60.4 %. As also, *IE* of the CS and CS/PEG nanoparticles were 65.8 % and 51.7 %, respectively (Table 1).

These results suggest that under the experimental conditions of this study, the CS/PEG interaction promotes the displacement of enzymatic molecules out of nanoparticles [46]. This could be justified by the intermolecular hydrogen bonding formed between the electronegative oxygen atom of PEG and the amino groups of chitosan. Therefore, the entanglement of PEG chains with chitosan molecules hinders the encapsulation of HRP in the nanoparticles by the steric repulsion mechanism [47,48].

In addition, PEG may interact with non-polar residues of the protein surface. This effect can be explained based on the hypothesis that high molecular weight PEG assumes a compact structure, caused by intramolecular hydrophobic interactions [49]. Thus, the presence of PEG in the nanoparticle composition increases the number of hydrophobic groups available for interaction with the enzyme, resulting in a worse enzymatic adhesion to the nanoparticles by steric exclusion [50].

3.3. FTIR spectra

The ability of the ionotropic gelation process to form CS NP and CS/PEG NP and to immobilize HRP was evaluated by FTIR. Spectra of materials, enzyme, and pure and charged nanoparticles are shown in Fig. 1.

In Fig. 1a, the CS spectra shows the strong and wide band in the area between 3500 – 3000 cm^{-1} as the result of the –OH stretching vibration associated with free, inter- and intra-molecular hydroxyl groups, superimposed primary amine N—H. Another characteristic band appears at 2875 cm^{-1}, attributed to the C–H stretch. The FTIR spectrum of chitosan also shows an amide bond band corresponding to the acetylated amine at 1653 cm^{-1} and a protonated amine band corresponding to the deacetylated amine at 1560 cm^{-1} obtained by the partial N-deacetylation of chitin [51], which is based on the results obtained in this study. The bands at 1420, 1375 and 1315 cm^{-1} are attributed to respective asymmetric deformations of C–H, C—N and CH_3 groups of acetamide remaining in the polymer chain, since the chitosan is not completely deacetylated. In addition, at 1150 cm^{-1}, another band is present due to C—O—C β- (1/4) and the band at 1025 cm^{-1} is attributed to the elongation of C—O, both of the glycopyranoside ring [52].

TPP spectra show two characteristic sharp peaks at 1134 cm^{-1} and 1095 cm^{-1} corresponding to symmetrical and anti-symmetric stretching vibrations of the O—P—O group and another at 887 cm^{-1}, referring to the anti-symmetric stretching of the P—O—P bridge [53]. In addition to these, we can see another peak at 1209 cm^{-1} attributed to P═O vibration of TPP [32].

In the CS NP spectra, the band between 3500 – 3000 cm^{-1} becomes wider and shifts to smaller wave numbers, indicating an increase of the hydrogen bonds [54]. In the nanoparticles, the 1560 cm^{-1} amine N—H flexion vibration bands and the 1655 cm^{-1} amide carbonyl stretch moved to 1540 cm^{-1} and 1636 cm^{-1}, respectively. The amine peak has its intensity increased by interaction with the PO- from TPP [55]. Moreover, in the spectra of CS NP, the bands at 1216 cm^{-1} and 887 cm^{-1} are observed regarding the vibrations of the P═O and P—O—P bonds of TPP. These results indicate the interaction between the amino groups of chitosan and the phosphate groups of TPP. It can be concluded that the appearance of these bands is an indication of the formation of nanoparticles and that the inter- and intra-molecular interactions are reinforced in chitosan nanoparticles [56].

Free HRP shows a typical spectrum with protein absorption bands associated with primary amide groups (corresponding to C═O

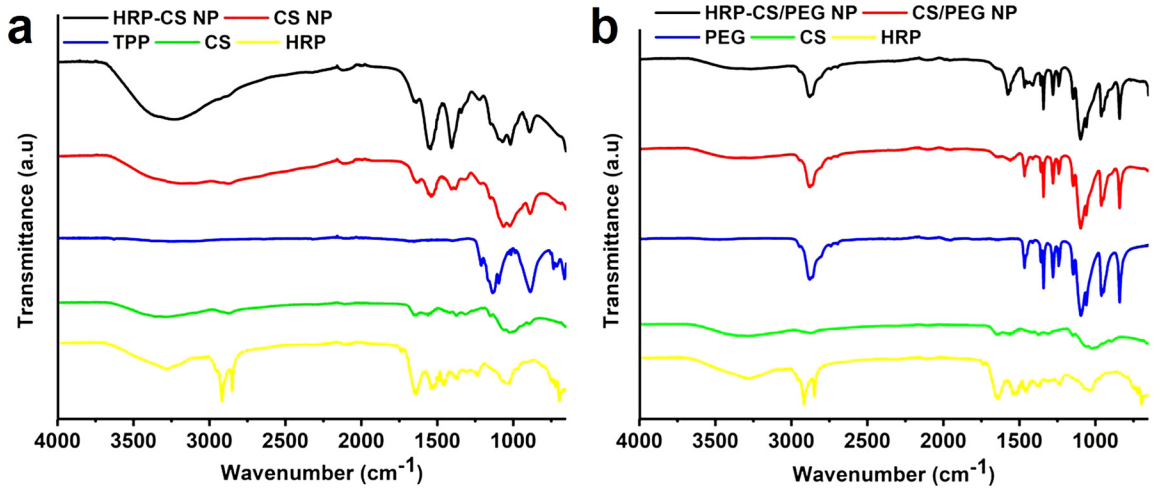

Fig. 1. Fourier transform infrared (FTIR) spectra. (a) Horseradish Peroxidase (HRP), Chitosan (CS), Sodium tripolyphosphate (TPP), Chitosan nanoparticles (CS NP) and HRP-loaded chitosan nanoparticles (HRP-CS NP); (b) HRP, CS, Polyethylene glycol (PEG), Chitosan/Polyethylene glycol nanoparticles (CS/PEG NP) and HRP-loaded Chitosan/Polyethylene glycol nanoparticles (HRP-CS/PEG NP).

elongation) at 1540 cm^{-1}, and secondary amide (attributed to N—H flexing and C—N elongation) [57,33]. It is also possible to observe characteristic bands of tertiary amide (R − CONR'R") arising from peptide bonds including proline residues between 1229 and 1337 cm^{-1} [58]. The absorption bands between 1350 and 1450 cm^{-1} can be attributed to the modes of heme vibration [59].

The spectrum of HRP-CS NP shows a reappearance of a broadband in the range of 3100 − 3550 cm^{-1} which may correspond to the additional hydrogen bonds between the chitosan and the enzyme, in addition to the overlap of the group N—H of the inserted HRP protein structure. There was also a clear increase in the intensities of the 1554 cm^{-1} and 1240 cm^{-1} bands belonging to the amide I and amide III stretching respectively, which can also be attributed to the HRP in HRP-CS NP [33]. The band corresponding to amide II is superimposed on that of chitosan after encapsulation, visualized by a slight peak around 1650 cm^{-1}.

In the Fig. 1b, characteristic bands of PEG at 1466 cm^{-1} and 1095 cm^{-1} (elongation at the ether bond) and 2879 cm^{-1} (C–H elongation) appear to be more intense than those of chitosan [59,60]. In addition, other typical PEG bands predominate in the spectrum of the CS/PEG NP due to the fact that PEG has a predilection for the particle surface, or because the absolute amount of PEG used in the preparation of NP is higher than that of chitosan. Despite this, a 1540 cm^{-1} band (NH flexion vibration) and the 1636 cm^{-1} amide carbonyl stretch appear on the spectrum of CS/PEG NP, a fact that does not occur in the pure PEG spectrum. In addition, the reappearance of the broadband in the area between 3500 − 3000 cm^{-1} corresponding to the hydrogen bonds, suggesting interactions between PEG and chitosan in the constitution of the nanoparticle [61].

Besides, the band at 1576 cm^{-1} also shows an amide II in HRP-CS/PEG NP [62]. It can also visualize a band overlap around 1400 cm^{-1}, which can be attributed to the heme group of peroxidase. The bands corresponding to amide III are suppressed in the spectrum of the nanoparticles of HRP-CS/PEG NP as a result of the presence of stronger bands attributed to PEG pools. These results suggest the presence of HRP in both nanoparticles, indicating that the essential characteristic of the native HRP structure did not change after the encapsulation in the nanoparticles [59].

3.4. Thermal analysis

TGA is a technique usually employed for the analysis of the decomposition and thermal stability of materials. This technique is capable to measure the weight change as a function of temperature [34]. All curves of TG and DTG can be observed in the Fig. 2. The curves in Fig. 2a and 2c showed that chitosan sample is degraded in a three-stage process. The first stage occurred between 35 and 100 °C, resulting from the removal of water, corresponding to a mass loss of more than 10 %. The second tipping point of the temperature range around 300 °C, characteristic of deacetylation, dehydration of saccharide rings and partial depolymerization of the chitosan chain, corresponding to approximately 50 % of the material mass. Similar results were observed by Kulig et al. [63]. The third inflection point occurred from 300 °C and extends to 500 °C, with mass loss of about 30 % of the total sample weight.

TG thermograms of CS NP before and after HRP immobilization are smooth with nearly similar behaviors of their decomposition. CS NP demonstrates three regular transition states. The first stage may due to physically adsorbed inter- and intra-molecular humidity up to 200 °C (DTG peak at 56 °C and 142 °C) that represents about 15 % of polymer weight. Where the second depression of samples weight begin from 230 to 350 °C (DTG peak at 261 °C) was attributed to the thermal decomposition of functional groups, such as CO, OH and NH_2, from pyranose ring along polymer backbone to form complex adduct (~15 % of polymer mass). The third decomposition occurs between 400 and 500 °C (DTG peak at 454 °C) attributed to thermal decomposition obtained from adducts (~20 % of weight) [64–66].

A similar profile was observed to HRP-CS NP. After immobilization of HRP, the DTG peaks were observed at 51 °C and 141 °C (first stage), 260 °C (second stage) and 452 °C (third stage), with global weight loss higher than CS NP. Thus, this thermal shift can be associated with the presence of HRP into nanomaterials. On the other hand, the residual mass of HRP-CS NP was slightly lesser in comparison with pure CS NP, suggesting the presence of enzyme into nanoparticles [67]. The higher final mass to both nanoparticles when compared to pure chitosan corresponds to the retention of residual ions from TPP cross-linking, as pure salt shows minimal mass loss after heating to the maximum study temperature [68].

Fig. 2b and 2d shows that pure PEG thermogram exhibit only one degradation stage from 250 °C to 420 °C, causing almost 100 % mass loss. This result is compatible with Kanis et al. [69]. An important weight loss is observed in CS/PEG NP between 180 °C and 220 °C and there is almost no weight loss below 180 °C. This can be attributed to the evaporation of water and organic components, similarly to has been observed to CS NP, even after blend formation [66]. Both CS/PEG NP and HRP-CS/PEG NP show a substantial weight loss between 390 °C and 420 °C (DTG peak at 407 °C and 410 °C, respectively), corresponding to the pyrolysis of PEG functional groups. This stage represents a significant weight loss of almost 70 % for CS/PEG NP and 90 % for HRP-CS/PEG NP. Furthermore, the residual mass was from 9.09 % to CS/PEG NP and 0.57 % to HRP-CS/PEG NP, indicating that the difference of weight loss can confirm the decomposition of the enzyme [34].

Sok and Fragoso [70] also observed mass loss below 520 °C (50 %), corresponding to the decomposition of immobilized HRP in modified carbon nanotubes. The authors also point out that the immobilized enzymes presented, in general, higher thermal stability when compared to the free enzyme, confirm the positive effect of immobilization on the enzyme stability [70].

Differential scanning calorimetry is used to determine any change in the physicochemical properties of the materials by measuring the energy transfer [71]. To confirm the physical state and interaction of the HRP in the CS and CS/PEG nanoparticles, the pure nanoparticles, free HRP, chitosan, PEG and HRP loaded into CS and CS/PEG nanoparticles were examined by DSC. The results were given in Fig. 3.

In Fig. 3a, DSC spectrum of chitosan shows a broad endothermic peak around 90 °C (between 60 °C and 140 °C) that may associate to dehydration of water content associated with the hydrophilic groups of CS. Chitosan exhibit exothermic band at 305 °C, that corresponding to pyranose ring thermal decomposition [64,71,72].

An acute endothermic peak was found at 57 °C in association with a large endothermic peak at 115 °C to CS NP, suggesting the increase in the thermal stability of the nanomaterial [73]. Two new endothermic peaks appear around 232 °C and 280 °C. The first one is possibly related to the breakdown of weak nonspecific electrostatic interactions, while the second one is associated with the breakdown of electrostatic bonds between the polymer and anion [74]. A new endothermic peak also appears around 326 °C to CS NP, indicating a change in the thermal nature of chitosan after reticulation. DSC spectrum of tripolyphosphate does not show any characteristic events of wide amplitude, besides a maximum temperature peak at 119 °C [72], without causing direct interference on the prepared nanoparticle spectrum.

After HRP immobilization, the endothermic peak at 57 °C in CS NP shown an increase of intensity in HRP-CS NP. Furthermore, a peak at 326 °C in the empty CS NP was shifted to 328 °C and presents either an increase of intensity. These changes support the interaction between HRP and CS NP.

Fig. 3b shows the DSC thermograms of the materials used to form CS/PEG nanoparticles and the immobilization of HRP into this particle. DSC curve of PEG shows a melting endothermic peak at 62 °C [34], and an exothermic peak of decomposition between 350 and 450 °C. In other hand, the observed decrease in the endothermic peak for CS/PEG nanoparticles when compared to pure PEG supports interaction between

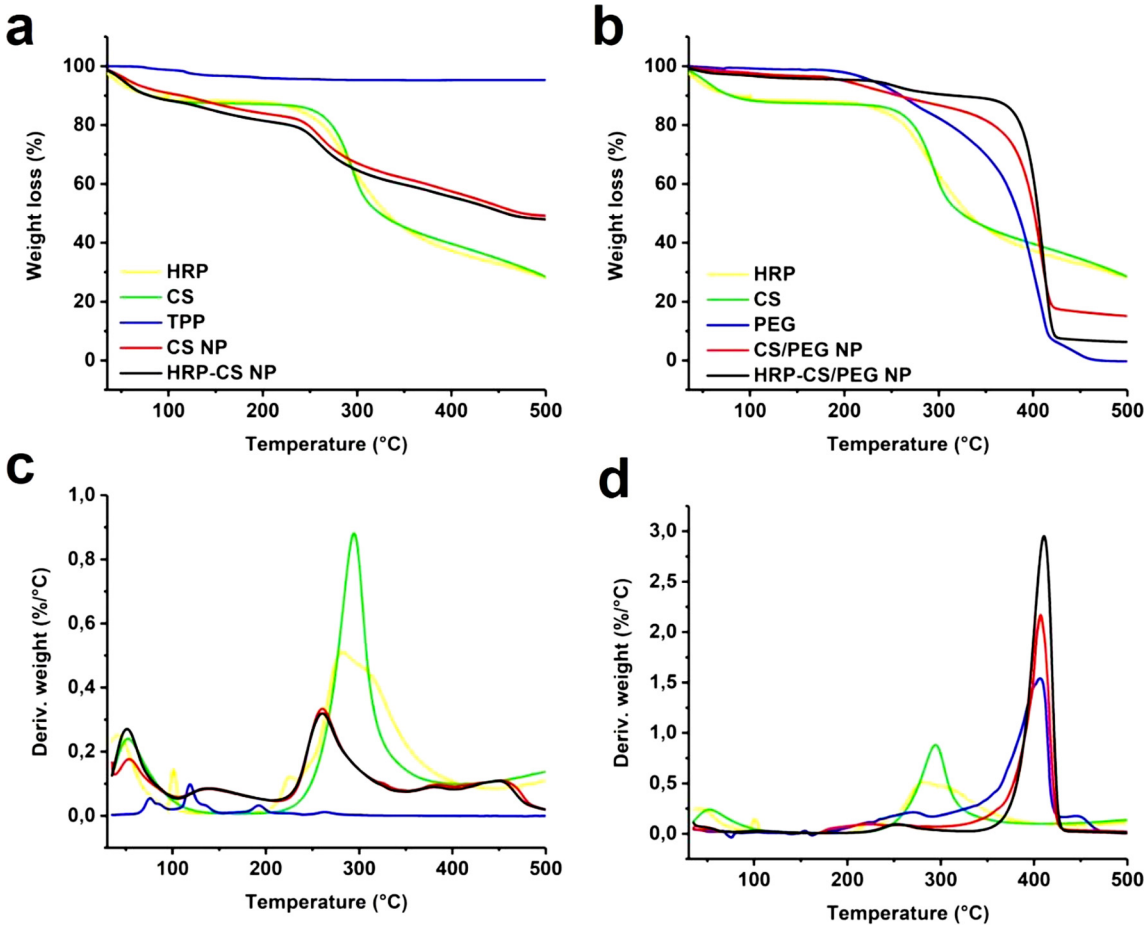

Fig. 2. Thermogravimetric (TG) curves. (a) Horseradish Peroxidase (HRP), Chitosan (CS), Sodium tripolyphosphate (TPP), Chitosan nanoparticles (CS NP) and HRP-loaded chitosan nanoparticles (HRP-CS NP); (b) HRP, CS, Polyethylene glycol (PEG), Chitosan/Polyethylene glycol nanoparticles (CS/PEG NP) and HRP-loaded Chitosan/Polyethylene glycol nanoparticles (HRP-CS/PEG NP); and their respective Derivative thermogravimetry (DTG) curves (c) and (d).

CS and PEG [60], in addition to the presence of an uniform exothermic peak of decomposition around 400 °C. HRP-CS/PEG NP thermogram showed the maintenance of the melting endothermic peak at 62 °C. Also, a change in peak presentation at 425 °C as a consequence of the interaction between the enzyme and the nanomaterial can be observed, which alters the nanoparticle decomposition profile. These results are compatible with the thermal decomposition profiles by TGA observed for these same materials in this work.

3.5. Morphology study of nanoparticles by SEM

The surface characterization of chitosan ad chitosan/PEG nanoparticles with and without immobilized HRP enzyme were carried out by Scanning Electron Microscopy (SEM), and results are exhibited in

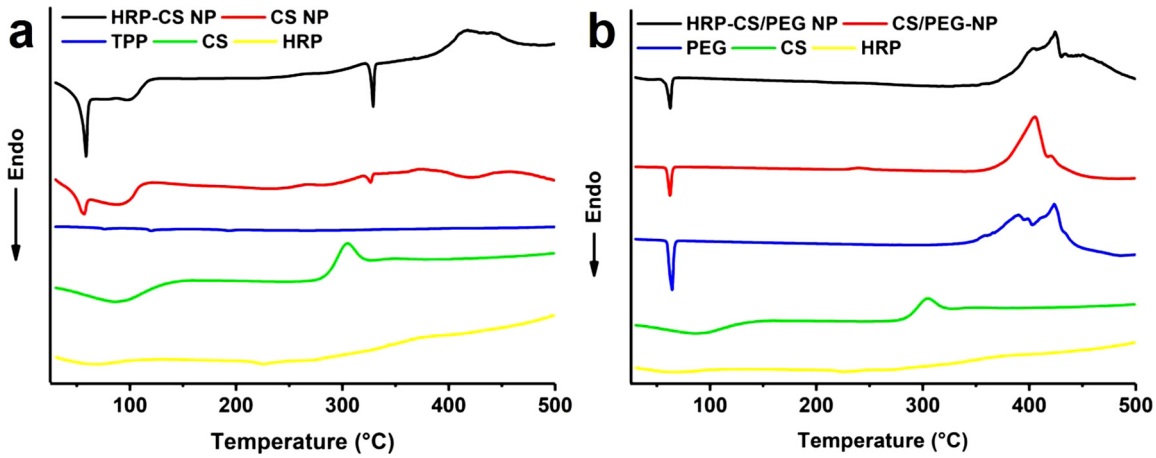

Fig. 3. Differential scanning calorimetry (DSC) spectra. (a) Horseradish Peroxidase (HRP), Chitosan (CS), Sodium tripolyphosphate (TPP), Chitosan nanoparticles (CS NP) and HRP-loaded chitosan nanoparticles (HRP-CS NP); and (b) HRP, CS, Polyethylene glycol (PEG), Chitosan/Polyethylene glycol nanoparticles (CS/PEG NP) and HRP-loaded Chitosan/Polyethylene glycol nanoparticles (HRP-CS/PEG NP).

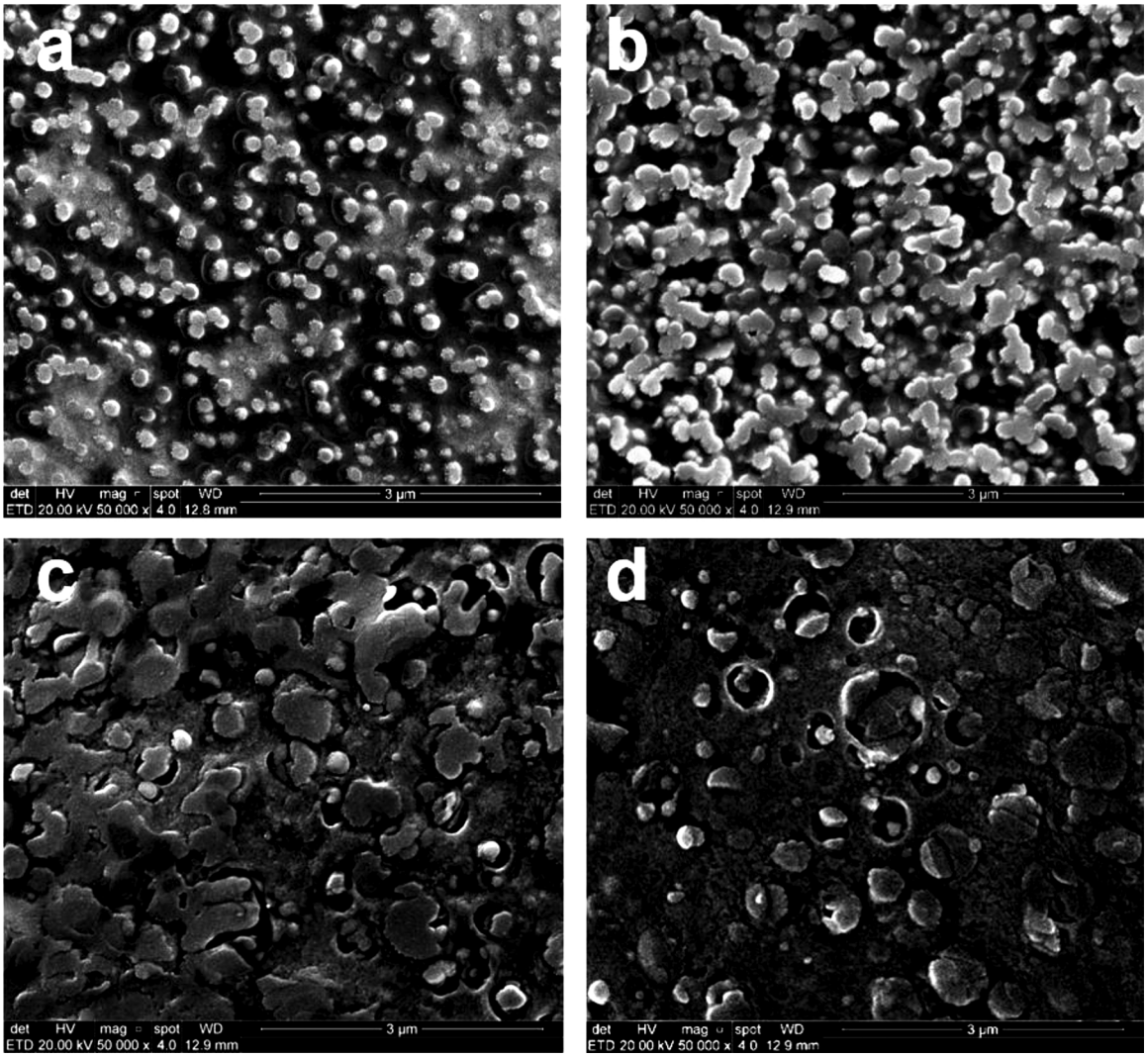

Fig. 4. Scanning electron microscopy (SEM) images. (a) Chitosan nanoparticles (CS NP); (b) HRP-loaded chitosan nanoparticles (HRP-CS NP); (c) Chitosan/Polyethylene glycol nanoparticles (CS/PEG NP); (d) HRP-loaded Chitosan/Polyethylene glycol nanoparticles (HRP-CS/PEG NP).

Fig. 4.

In Fig. 4a, CS nanoparticles were found to be roughly homogeneous spherical in shape with a smooth surface and demonstrate average size diameters with narrow size distributions. Similar observations were made by Rostami et al. [75], Agarwal et al. [76] and Mariadoss et al. [77] when analyzing chitosan nanoparticles prepared by ionotropic gelation by SEM. Similar characteristics can be found to HRP-CS NP (Fig. 4b).

Furthermore, the incorporation of PEG in the CS produced a compact structure in both CS/PEG (Fig. 4c) and HRP-CS/PEG (Fig. 4d) nanoparticles, similar to a coating layer due to the higher PEG amount in the preparation process of the nanoparticles besides the appearance of pores resulting from the dehydration process applied for the microscopy analysis. The formation of a compact material was also observed by Khoee et. al. [78] after coating of iron oxide nanoparticles with high molar ratios of poly-ε-caprolactone and PEG.

In this study, nanoparticles containing PEG kept a larger diameter in comparison to nanoparticles without this polymer when measured by the SEM ruler (data not shown), as evidenced by the dynamic light scattering technique. In addition, some aggregates were observed when nanoparticles were composed with PEG. This constatation can be attributed to the anionic characteristic of this polymer, which decreases the total charge of nanoparticles. Similar observation was made by Elwerfalli et al. [71] studying the influence of various polymers on the coating of chitosan nanoparticles.

3.6. Biochemical analysis

3.6.1. Effect of temperature and pH on HRP activity

The optimum temperature of the immobilized enzymes tends to be directed towards higher temperatures when compared to the free enzymes. During enzymatic immobilization, the free circulation of enzyme molecules is obstructed, even at higher temperatures. Thus, enzymatic denaturation is less observed due to amino acid protection, while the conversion of the substrate continues at higher temperatures. In addition, as the temperature increases, the substrate molecules gain kinetic energy and reach the active site of the immobilized enzyme rapidly. The extent of the optimal temperature shift for immobilized enzymes depends on the type of matrix as well as on the interactions between the enzyme and the matrix [79]. Therefore, the effect of temperature variation on the activity of free HRP and HRP encapsulated in CS and CS/PEG nanoparticles was studied. Fig. 5 shows the relative activity of HRP when the reaction occurs in different temperatures (25–65 °C).

In this study, the optimal temperature for free HRP was 40 °C, similar to the value found in the literature [80]. The optimum temperature for encapsulated HRP was 45 °C for both nanoparticles, with slightly higher results for HRP-CS NP, which maintained its activity

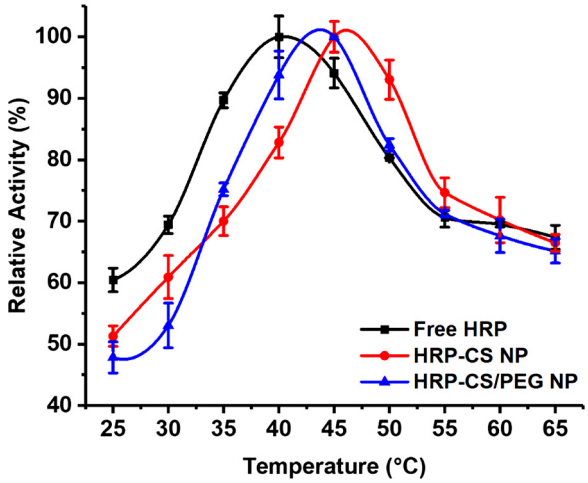

Fig. 5. Effect of temperature (25-65 °C) on activity of free Horseradish Peroxidase (HRP), HRP-loaded chitosan nanoparticles (HRP-CS NP) and HRP-loaded Chitosan/Polyethylene glycol nanoparticles (HRP-CS/PEG NP). Maximal activity -100 %: 133.76 ± 3.14 U/mg (HRP); 188.31 ± 6.67 U/mg (HRP-CS NP); 152.12 ± 14.8 U/mg (HRP-CS/PEG NP). According to the enzyme activity assay methodology.

above 90 % at 50 °C. The possibility of hydrogen bonds and hydrophobic interactions HRP-PEG, in addition to the decreasing the adhesion of the enzyme [50], can to result in decrease of the activity of the immobilized enzyme by accelerate structural changes on the enzyme with the increase of the temperature. The increment of the optimum temperature for HRP immobilized on both nanostructures is consistent with those obtained by Monier et al. [62], which observed an optimum temperature of 45 °C for HRP immobilized on polyethylacrylate grafted chitosan granules, with high residual activity at temperatures above the optimum (up to 55 °C). Gupta et al. [81] obtained increased activity of HRP immobilized on silica nanoparticles containing gadolinium oxide up to 60 °C. Abdulaal et al. [12], Mohamed et al. [82], and Yu et al. [83] also observed the increase in the optimal temperature of HRP after immobilization onto Fe_3O_4 nanoparticle–polymethyl methacrylate film (from 30 to 40 °C), chitosan beads (from 35 to 45 °C), and amino-functionalized bacterial cellulose (from 25 to 30 °C), respectively.

The fact that the encapsulated enzyme has an optimal temperature above the free enzyme is due to the fact that the interactions of HRP to the CS and CS/PEG nanoparticles increase the stabilization of the HRP molecule and, even at a higher temperature, the encapsulated HRP can maintain its active structure compared to the free enzyme. This may occur because the polymer matrix protects the encapsulated enzyme from heat and restricts its mobility against temperature-induced denaturation, thereby increasing its stability over a wider range of temperatures. This hypothesis is also affirmed by the cited authors [62,81].

The optimal pH of an enzyme is based on the pKa of amino acids in the vicinity of the active site of the enzyme. The change in the optimum pH can be observed when the enzymes are immobilized and can be amplified or moved to the acid or basic side, relative to the free enzyme [79]. The effect of pH variation on the activity of free and immobilized HRP in CS and CS/PEG nanoparticles was studied. Fig. 6 shows the relative activity of HRP when the reaction occurs in a media of different pH (4.0–9.0).

HRP encapsulated into both CS and CS/PEG nanoparticles showed a similar profile at different pH, with maximum activity at pH 7.0, similar to that of the free enzyme, as observed in recent works using different supports [8,27]. A gradual decrease from that point when the reaction medium approached extremes of acidity or alkalinity was also observed. Similar to that observed with the temperature variation, HRP-CS NP showed slightly higher results than free HRP and HRP-CS/PEG NP, which maintained its activity close to 70 % even in the highly alkaline reaction medium (pH 9). The same profile was observed by the authors previously mentioned.

The immobilized HRP microenvironment and buffer solution may have uneven partitioning of H^+ and OH^- concentrations due to both electrostatic interactions with the cationic polymer matrix of chitosan. The decrease in H^+ diffusion to the enzymatic microenvironment results in a significant difference between the pH of the two environments, guaranteeing the enzyme less exposure to more extreme pH by the protection of the polymer support [62].

The extent of the change depends on the type of immobilization method used, as well as on the physical and chemical properties of the matrix. When the matrix is positively charged, as is the case for CS NP, it leads to the repulsion of the protons, whereas the attraction of electrons changes the optimal pH towards the basic side [79]. Despite not changing the optimum pH in comparison with HRP-CS/PEG NP, HRP-CS NP, which presents a more positive surface charge, tend to support better activities in a more alkaline environment.

Due the charged polymer nanoparticles cause a partition of protons between the reaction medium and the enzyme microenvironment, the curve of the pH profile of the entrapped enzyme tends to be wider than that of the free enzyme. This shows that the encapsulated enzyme is more resistant to changes in pH-dependent activity than the free enzyme as a result of being trapped inside the polymer matrix, which acts as a protection for the immobilized enzyme [81].

3.6.2. Study of kinetic parameters

The understanding of kinetic parameters of the enzyme is fundamental for the evaluation of the enzymatic activity after the immobilization processes. The three most relevant kinetic parameters in this evaluation are K_M, V_{max}, and K_{cat}. V_{max}, or maximum velocity, denotes the maximum rate of an enzymatic reaction, while K_M, or Michaelis constant, represents the concentration of substrate capable of reaching half the V_{max} of the reaction, denoting the degree of affinity of the enzyme for the substrate. K_{cat}, or catalytic constant, determines the rate limiting the reaction catalyzed by an enzyme under saturation conditions and can be calculated from the division between the V_{max} and the initial concentration of enzyme offered in the reaction ($[E]_0$) [84].

Changes in kinetic parameters are observed during enzymatic immobilization. Enzymatic immobilization does not ensure that the enzyme molecules are bound in their correct conformation, which strongly affects the V_{max} of the enzyme. In addition, diffusion barriers are other important reasons for changes in kinetic parameters, especially K_M. In the case of an internal diffusion barrier, the enzyme is present inside the matrix, which limits the diffusion of substrate molecules to the matrix, which affects K_M followed by V_{max}. Thus, it becomes important to quantify the diffusion constant (K_α) from the V_{max}/K_M ratio. Finally, to determine the catalytic efficiency of an enzymatic reaction, one must analyze the specific constant (K_e), defined as K_{cat}/K_M [79].

Lineweaver-Burk double reciprocal plots and calculated kinetic parameters from free HRP and HRP immobilized into CS and CS/PEG nanoparticles are shown in Fig. 7 and Table 2. The calculated values of K_M for HRP encapsulated into CS and CS/PEG nanoparticles were 18.28 and 19.92 mM, respectively. These values were higher than those found for free HRP (17.78 mM). HRP encapsulated into CS nanoparticles did not present statistically significant differences when compared to free HRP, while HRP encapsulated into CS/PEG NP were statistically higher than free enzyme and HRP-CS NP ($p < 0.001$).

On the other hand, the calculated values of V_{max} of the enzyme encapsulated by CS and CS/PEG nanoparticles were 3.82 and 4.11 mM/min, respectively. These values of maximum speed were both statistically lower than the free enzyme (5.07 mM/min) ($p < 0.001$) and present statistical difference between them ($p < 0.05$). All other parameters studied (K_{cat}, K_α and K_e) showed a statistically significant reduction in comparison with the free enzyme ($p < 0.001$), indicating

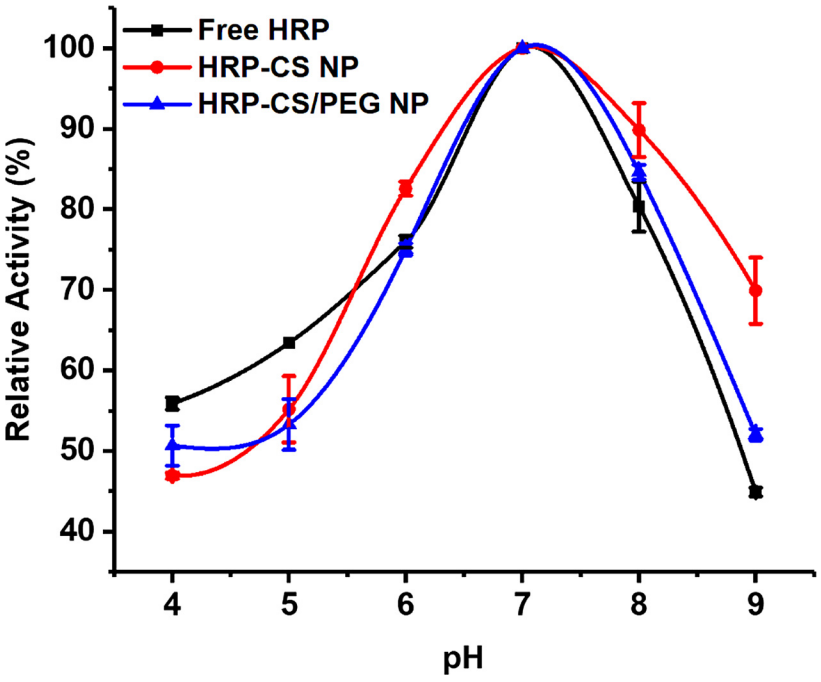

Fig. 6. Effect of pH (4,0 - 9,0) on activity of free Horseradish Peroxidase (HRP), HRP-loaded chitosan nanoparticles (HRP-CS NP) and HRP-loaded Chitosan/Polyethylene glycol nanoparticles (HRP-CS/PEG NP). Maximal activity -100 %: 161.09 ± 20.9 U/mg (HRP); 55.94 ± 8.94 U/mg (HRP-CS NP); 61.56 ± 2.15 U/mg (HRP-CS/PEG NP). According to the enzyme activity assay methodology.

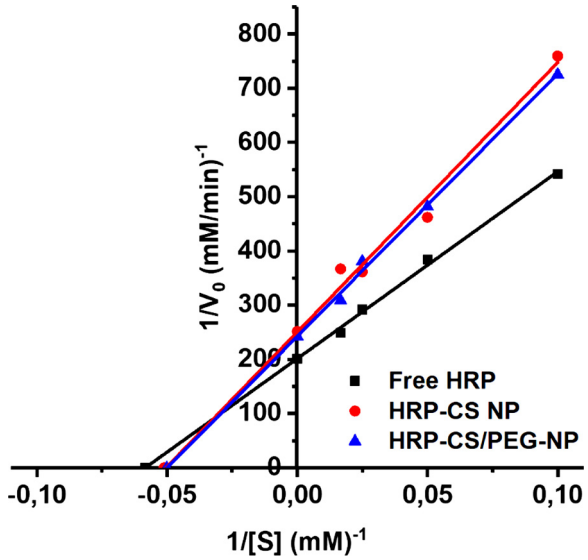

Fig. 7. Lineweaver-Burk plots for kinetic parameters determination of free Horseradish Peroxidase (HRP), HRP-loaded chitosan nanoparticles (HRP-CS NP) and HRP-loaded Chitosan/Polyethylene glycol nanoparticles (HRP-CS/PEG NP). Substrates concentration: Guaiacol (10 to 100 mM) and H_2O_2 2 mM. According to the enzyme activity assay methodology.

a relative decrease in enzymatic kinetics after the encapsulation process.

The change in the kinetic parameters of the enzyme in the nanoparticles may be due to changes in the microenvironment or conformation of the enzyme after encapsulation [85]. This behavior occurs by the limitation in the mass transfer of the substrate through the reticulated network of chitosan or some possible steric hindrance due to the structural rigidity of the enzymatic structure distorted after encapsulation [62], or due to the highly hydrophilic repulsive layer of PEG, reducing the guaiacol diffusion to the inside of the nanoparticle.

Gupta et al. [81] and Chiu et al. [86] when studying the immobilization of HRP enzyme on silica nanoparticles also observed higher values of K_M for immobilized HRP. Monier et al. [62] and Spasojević et al. [80] also obtained similar behaviors with HRP immobilized on chitosan and alginate granules, respectively.

The comparison of the kinetic parameters studied indicates that both encapsulated HRP exhibit similar kinetics, and are not distant to that of free HRP, which values the encapsulation processes studied, indicating relative maintenance of the enzyme's affinity to the substrate even after encapsulation.

4. Conclusion

In summary, HRP was successfully immobilized into both chitosan and chitosan/PEG nanoparticles, presenting better immobilization results in the absence of PEG. All particles presented small sizes between 135 and 229 nm, positive surface charges in a range of +20 to +28 mV and spherical profile. Morphological, physicochemical and thermal

Table 2
Kinetic parameters values for free Horseradish Peroxidase (Free HRP), HRP-loaded chitosan nanoparticles (HRP-CS NP) and HRP-loaded Chitosan/Polyethylene glycol nanoparticles (HRP-CS/PEG NP).

Sample	Kinetic Parameters				
	V_{max} (mM/min)	K_M (mM)	K_{cat} (min^{-1})	K_α (min^{-1})	K_e ($mM^{-1}\,min^{-1}$)
Free HRP	5.07 ± 0.11	17.78 ± 0.68	87.78 ± 1.91	0.27 ± 0.02	4.94 ± 0.08
HRP-CS NP	3.82 ± 0.15	18.28 ± 1.28	66.10 ± 2.65	0.21 ± 0.01	3.62 ± 0.11
HRP-CS/PEG NP	4.11 ± 0.01	19.92 ± 0.04	71.19 ± 0.15	0.20 ± 0.01	3.57 ± 0.01

characterizations indicated the formation of nanoparticles and confirmed the HRP immobilization. The optimal temperature from immobilized HRP was higher than free enzyme, increasing from 40 °C to 45 °C, and the optimal pH of 7.0 has not changed after HRP immobilization. The analysis of kinetic parameters showed similar results for HRP immobilized into both chitosan and chitosan/PEG nanoparticles when compared to free HRP. Thus, both nanoparticles are capable of immobilizing HRP without affect significantly its biochemical properties and the addition of polyethylene glycol did not represent an advantage in terms of enzymatic kinetics for HRP immobilized into chitosan nanoparticles. Chitosan nanoparticles in the absence or presence of PEG represents promising supports for different uses of HRP in the future, including for biomedical applications.

CRediT authorship contribution statement

Micael Nunes Melo: Conceptualization, Methodology, Validation, Formal analysis, Investigation, Writing - original draft. **Fernanda Menezes Pereira:** Methodology, Investigation. **Matheus Alves Rocha:** Methodology, Investigation. **Jesica Gonçalves Ribeiro:** Methodology, Investigation. **Fernando Mendonça Diz:** Validation. **Wesley Formentin Monteiro:** Investigation, Writing - review & editing. **Rosane Angélica Ligabue:** Supervision, Writing - review & editing. **Patrícia Severino:** Supervision, Writing - review & editing. **Alini Tinoco Fricks:** Supervision, Conceptualization, Resources, Project administration, Funding acquisition.

Declaration of Competing Interest

The authors report no declarations of interest.

Acknowledgements

The Authors are grateful for the financial support from the Brazilian research funding agencies CAPES, CNPq and FAPITEC/SE.

Appendix A. Supplementary data

Supplementary material related to this article can be found, in the online version, at doi:https://doi.org/10.1016/j.procbio.2020.08.007.

References

[1] L.C. Lopes, M.T.M. Barreto, K.M. Gonçalves, H.M. Alvarez, M.F. Heredia, R.O.M.A. de Souza, Y. Cordeiro, C. Dariva, A.T. Fricks, Stability and structural changes of horseradish peroxidase: microwave versus conventional heating treatment, Enzyme Microb. Technol. 69 (2015) 10–18, https://doi.org/10.1016/j.enzmictec.2014.11.002.

[2] D.I. Colpa, M.W. Fraaije, E. Van Bloois, DyP-type peroxidases: a promising and versatile class of enzymes, J. Ind. Microbiol. Biotechnol. 41 (1) (2013) 1–7, https://doi.org/10.1007/s10295-013-1371-6.

[3] H. Yang, C. Gong, L. Miao, F. Xu, A glucose biosensor based on horseradish peroxidase and glucose oxidase Co-entrapped in carbon nanotubes modified electrode, Int. J. Electrochem. Sci. 12 (6) (2017) 4958–4969, https://doi.org/10.20964/2017.06.05.

[4] T.T. Ngo, Peroxidase in chemical and biochemical analysis, Anal. Lett. 43 (10-11) (2010) 1572–1587, https://doi.org/10.1080/00032711003653874.

[5] G.R. Lopes, D.C.G.A. Pinto, A.M.S. Silva, Horseradish peroxidase (HRP) as a tool in green chemistry, RSC Adv. 4 (70) (2014) 37244–37265, https://doi.org/10.1039/c4ra06094f.

[6] N.Ž. Šekuljica, N.Ž. Prlainović, A.B. Stefanović, M.G. Žuža, D.Z. Čičkarić, D.Ž. Mijin, Z.D. Knežević-Jugović, Decolorization of anthraquinonic dyes from textile effluent using horseradish peroxidase: optimization and kinetic study, Sci. World J. 2015 (2015) 1–12, https://doi.org/10.1155/2015/371625.

[7] F. Zhang, W. Zhang, L. Zhao, H. Liu, Degradation of phenol with Horseradish Peroxidase immobilized on ZnO nanocrystals under combined irradiation of microwaves and ultrasound, Desalin. Water Treat. 57 (51) (2016) 24406–24416, https://doi.org/10.1080/19443994.2016.1138886.

[8] J. Li, X. Chen, D. Xu, K. Pan, Immobilization of horseradish peroxidase on electrospun magnetic nanofibers for phenol removal, Ecotoxicol. Environ. Saf. 170 (2019) 716–721, https://doi.org/10.1016/j.ecoenv.2018.12.043.

[9] Y. Chung, Y. Kwon, Glucose biofuel cells using bi-enzyme catalysts including glucose oxidase, horseradish peroxidase and terephthalaldehyde crosslinker, Chem. Eng. J. 334 (2018) 1085–1092, https://doi.org/10.1016/j.cej.2017.10.121.

[10] J.W. Bae, J.H. Choi, Y. Lee, K.D. Park, Horseradish peroxidase-catalysedin situ-forming hydrogels for tissue-engineering applications, J. Tissue Eng. Regen. Med. 9 (11) (2014) 1225–1232, https://doi.org/10.1002/term.1917.

[11] G. Bonifert, L. Folkes, C. Gmeiner, G. Dachs, O. Spadiut, Recombinant horseradish peroxidase variants for targeted cancer treatment, Cancer Med. 5 (6) (2016) 1194–1203, https://doi.org/10.1002/cam4.668.

[12] W.H. Abdulaal, Y.Q. Almulaiky, R.M. El-Shishtawy, Encapsulation of HRP enzyme onto a magnetic Fe_3O_4 Np–PMMA film via casting with sustainable biocatalytic activity, Catalysts. 10 (2) (2020), https://doi.org/10.3390/catal10020181 181.

[13] C. Mateo, J.M. Palomo, G. Fernandez-Lorente, J.M. Guisan, R. Fernandez-Lafuente, Improvement of enzyme activity, stability and selectivity via immobilization techniques, Enzyme Microb. Technol. 40 (2007) 1451–1463, https://doi.org/10.1016/j.enzmictec.2007.01.018.

[14] M. Aldhahri, Y.Q. Almulaiky, R.M. El-Shishtawy, W.M. Al-Shawafi, N. Salah, A. Alshahrie, H.A.H. Alzahrani, Ultra-thin 2D CuO nanosheet for HRP immobilization supported by encapsulation in a polymer matrix: characterization and dye degradation, Catal. Letters (2020), https://doi.org/10.1007/s10562-020-03289-7.

[15] W.M. Alshawafi, M. Aldhahri, Y.Q. Almulaiky, N. Salah, S.S. Moselhy, I.H. Ibrahim, S.A. Mohamed, Immobilization of horseradish peroxidase on PMMA nanofibers incorporated with nanodiamond, Artif. Cells Nanomed. Biotechnol. 46 (sup3) (2018) S973–S981, https://doi.org/10.1080/21691401.2018.1522321.

[16] S.A. Mohamed, M.H. Al-Harbi, Y.Q. Almulaiky, I.H. Ibrahim, R.M. El-Shishtawy, Immobilization of horseradish peroxidase on Fe_3O_4 magnetic nanoparticles, Electron. J. Biotechnol. 27 (2017) 84–90, https://doi.org/10.1016/j.ejbt.2017.03.010.

[17] A. Arsalan, H. Younus, Enzymes and nanoparticles: Modulation of enzymatic activity via nanoparticles, Int. J. Biol. Macromol. 118 (B) (2018) 1833–1847, https://doi.org/10.1016/j.ijbiomac.2018.07.030.

[18] H. Mo, J. Qiu, C. Yang, L. Zang, E. Sakai, J. Chen, Porous biochar/chitosan composites for high performance cellulase immobilization by glutaraldehyde, Enzyme Microb. Technol. 138 (2020) 109561, https://doi.org/10.1016/j.enzmictec.2020.109561.

[19] A. Baranwal, A. Kumar, A. Priyadharshini, G.S. Oggu, I. Bhatnagar, A. Srivastava, P. Chandra, Chitosan: An undisputed bio-fabrication material for tissue engineering and bio-sensing applications, Int, J. Biol. Macromol. 110 (2018) 110–123, https://doi.org/10.1016/j.ijbiomac.2018.01.006.

[20] D. Wang, W. Jiang, Preparation of chitosan-based nanoparticles for enzyme immobilization, Int. J. Biol. Macromol. 126 (2019) 1125–1132, https://doi.org/10.1016/j.ijbiomac.2018.12.243.

[21] M. Naghdi, M. Taheran, S.K. Brar, A. Kermanshahi-pour, M. Verma, R.Y. Surampalli, Fabrication of nanobiocatalyst using encapsulated laccase onto chitosan-nanobiochar composite, Int, J. Biol. Macromol. 124 (2019) 530–536, https://doi.org/10.1016/j.ijbiomac.2018.11.234.

[22] M. Leonida, S. Belbekhouche, F. Adams, U.K. Bijja, D.-A. Choudhary, I. Kumar, Enzyme nanovehicles: histaminase and catalase delivered in nanoparticulate chitosan, Int. J. Pharm. 557 (2019) 145–153, https://doi.org/10.1016/j.ijpharm.2018.12.050.

[23] T. Inanan, Chitosan Co-polymeric nanostructures for catalase immobilization, React. Funct. Polym. 135 (2019) 94–102, https://doi.org/10.1016/j.reactfunctpolym.2018.12.

[24] T. Kadri, A. Cuprys, T. Rouissi, S.K. Brar, R. Daghrir, J.-M. Lauzon, Nanoencapsulation and release study of enzymes from Alkanivorax borkumensis in chitosan-tripolyphosphate formulation, Biochem. Eng. J. 137 (2018) 1–10, https://doi.org/10.1016/j.bej.2018.05.013.

[25] M.N.M. Cunha, H.P. Felgueiras, I. Gouveia, A. Zille, Synergistically enhanced stability of laccase immobilized on synthesized silver nanoparticles with water-soluble polymers, Colloids Surf. B Biointerfaces 154 (2017) 210–220, https://doi.org/10.1016/j.colsurfb.2017.03.023.

[26] L. Guerrini, R. Alvarez-Puebla, N. Pazos-Perez, Surface modifications of nanoparticles for stability in biological fluids, Materials 11 (7) (2018) 1154, https://doi.org/10.3390/ma11071154.

[27] X. Xie, P. Luo, J. Han, T. Chen, Y. Wang, Y. Cai, Q. Liu, Horseradish peroxidase immobilized on the magnetic composite microspheres for high catalytic ability and operational stability, Enzyme Microb. Technol. 122 (2019) 26–35, https://doi.org/10.1016/j.enzmictec.2018.12.007.

[28] L.A. Frank, P.S. Chaves, C.M. D'Amore, R.V. Contri, A.G. Frank, R.C.R. Beck, S.S. Guterres, The use of chitosan as cationic coating or gel vehicle for polymeric nanocapsules: increasing penetration and adhesion of imiquimod in vaginal tissue, Eur. J. Pharm. Biopharm. 114 (2017) 202–212, https://doi.org/10.1016/j.ejpb.2017.01.021.

[29] L.A. Frank, G.R. Onzi, A.S. Morawski, A.R. Pohlmann, S.S. Guterres, R.V. Contri, Chitosan as a coating material for nanoparticles intended for biomedical applications, React. Funct. Polym. 147 (2020) 104459, https://doi.org/10.1016/j.reactfunctpolym.2019.104459.

[30] M.C.F. Gonçalves, O. Mertins, A.R. Pohlmann, N.P. Silveira, S.S. Guterres, Chitosan coated liposomes as an innovative nanocarrier for drugs, J. Biomed. Nanotechnol. 8 (2) (2012) 240–250, https://doi.org/10.1166/jbn.2012.1375.

[31] P. Calvo, C. Remuñán-López, J.L. Vila-Jato, M.J. Alonso, Novel hydrophilic chitosan-polyethylene oxide nanoparticles as protein carriers, J. Appl. Polym. Sci. 63 (1) (1997) 125–132, https://doi.org/10.1002/(sici)1097-4628(19970103)63:1<125::aid-app13>3.0.co;2-4.

[32] L.E. Scheeren, D.R. Nogueira, L.B. Macedo, M.P. Vinardell, M. Mitjans, M.R. Infante, C.M.B. Rolim, PEGylated and poloxamer-modified chitosan nanoparticles

incorporating a lysine-based surfactant for pH-triggered doxorubicin release, Colloids Surf. B Biointerfaces 138 (2016) 117–127, https://doi.org/10.1016/j.colsurfb.2015.11.049.
[33] N.K. Garg, P. Dwivedi, C. Campbell, R.K. Tyagi, Site specific/targeted delivery of gemcitabine through anisamide anchored chitosan/poly ethylene glycol nanoparticles: an improved understanding of lung cancer therapeutic intervention, Eur. J. Pharm. Sci. 47 (5) (2012) 1006–1014, https://doi.org/10.1016/j.ejps.2012.09.012.
[34] T. Jayaramudu, G.M. Raghavendra, K. Varaprasad, G.V.S. Reddy, A.B. Reddy, K. Sudhakar, E.R. Sadiku, Preparation and characterization of poly(ethylene glycol) stabilized nano silver particles by a mechanochemical assisted ball mill process, J. Appl. Polym. Sci. 133 (7) (2016) 43027, https://doi.org/10.1002/app.43027.
[35] T. Hirata, S. Izumi, M. Ogura, T. Yawata, Epoxidation of styrenes with the peroxidase from the cultured cells of Nicotiana tabacum, Tetrahedron Lett. 54 (52) (1998) 15993–16003, https://doi.org/10.1016/s0040-4020(98)01007-2.
[36] S. Kunjachan, S. Jose, Understanding the mechanism of ionic gelation for synthesis of chitosan nanoparticles using qualitative techniques, Asian J. Pharm. 4 (2) (2010) 148, https://doi.org/10.4103/0973-8398.68467.
[37] S. Bhattacharjee, DLS and zeta potential – what they are and what they are not? J. Control. Release 235 (2016) 337–351, https://doi.org/10.1016/j.jconrel.2016.06.017.
[38] C. Prego, D. Torres, E. Fernandez-Megia, R. Novoa-Carballal, E. Quiñoá, M.J. Alonso, Chitosan–PEG nanocapsules as new carriers for oral peptide delivery, J. Control. Release 111 (3) (2006) 299–308, https://doi.org/10.1016/j.jconrel.2005.12.015.
[39] Y. Xu, Y. Du, Effect of molecular structure of chitosan on protein delivery properties of chitosan nanoparticles, Int. J. Pharm. 250 (1) (2003) 215–226, https://doi.org/10.1016/s0378-5173(02)00548-3.
[40] X. Zhang, Nasal absorption enhancement of insulin using PEG-grafted chitosan nanoparticles, Eur. J. Pharm. Biopharm. 68 (3) (2008) 526–534, https://doi.org/10.1016/j.ejpb.2007.08.009.
[41] L.C.L. Novaes, A.F. Jozala, P.G. Mazzola, A.P. Júnior, The influence of pH, polyethylene glycol and polyacrylic acid on the stability of stem bromelain, Braz. J. Pharm. Sci. 50 (2) (2014) 371–380, https://doi.org/10.1590/s1984-82502014000200017.
[42] A.H. Najafabadi, M. Abdouss, S. Faghihi, Synthesis and evaluation of PEG-O-chitosan nanoparticles for delivery of poor water soluble drugs: ibuprofen, Mater. Sci. Eng. C. 41 (2014) 91–99, https://doi.org/10.1016/j.msec.2014.04.035.
[43] S. Tan, D. Gu, H. Liu, Q. Liu, Detection of a single enzyme molecule based on a solid-state nanopore sensor, Nanotechnology. 27 (15) (2016) 155502, https://doi.org/10.1088/0957-4484/27/15/155502.
[44] S.E. Rodríguez-deLuna, I.E. Moreno-Cortez, M.A. Garza-Navarro, R. Lucio-Porto, L. López Pavón, V.A. González-González, Thermal stability of the immobilization process of horseradish peroxidase in electrospun polymeric nanofibers, J. Appl. Polym. Sci. 134 (19) (2017) 44811, https://doi.org/10.1002/app.44811.
[45] C. Oliver, C.L. Tolbert, J.F. Waters, Internalization of horseradish peroxidase isozymes by pancreatic acinar cells in vitro, J. Histochem. Cytochem. 37 (1) (1989) 49–56, https://doi.org/10.1177/37.1.2908883.
[46] N. Sawtarie, Y. Cai, Y. Lapitsky, Preparation of chitosan/tripolyphosphate nanoparticles with highly tunable size and low polydispersity, Colloids Surf. B Biointerfaces 157 (2017) 110–117, https://doi.org/10.1016/j.colsurfb.2017.05.055.
[47] W.E. Rudzinski, A. Palacios, A. Ahmed, M.A. Lane, T.M. Aminabhavi, Targeted delivery of small interfering RNA to colon cancer cells using chitosan and PEGylated chitosan nanoparticles, Carbohydr. Polym. 147 (2016) 323–332, https://doi.org/10.1016/j.carbpol.2016.04.041.
[48] M. Nag, V. Gajbhiye, P. Kesharwani, N.K. Jain, Transferrin functionalized chitosan-PEG nanoparticles for targeted delivery of paclitaxel to cancer cells, Colloids Surf. B Biointerfaces 148 (2016) 363–370, https://doi.org/10.1016/j.colsurfb.2016.08.059.
[49] A. Jain, K. Thakur, G. Sharma, P. Kush, U.K. Jain, Fabrication, characterization and cytotoxicity studies of ionically cross-linked docetaxel loaded chitosan nanoparticles, Carbohydr. Polym. 137 (2016) 65–74, https://doi.org/10.1016/j.carbpol.2015.10.012.
[50] G. Liu, Y. Lin, V. Ostatná, J. Wang, Enzyme nanoparticles-based electronic biosensor, ChemComm. (27) (2005) 3481, https://doi.org/10.1039/b504943a.
[51] B. Sarmento, D. Ferreira, F. Veiga, A. Ribeiro, Characterization of insulin-loaded alginate nanoparticles produced by ionotropic pre-gelation through DSC and FTIR studies, Carbohydr. Polym. 66 (1) (2006) 1–7, https://doi.org/10.1016/j.carbpol.2006.02.008.
[52] J.N. Silva, M.C. Bezerra, P.M.A. Farias, Novel and simple route for the synthesis of core–shell chitosan–gold nanocomposites, Mater. Chem. Phys. 135 (1) (2012) 63–67, https://doi.org/10.1016/j.matchemphys.2012.04.01.
[53] M.M. Badran, G.I. Harisa, S.A. AlQahtani, F.K. Alanazi, K.M.A. Zoheir, Pravastatin-loaded chitosan nanoparticles: formulation, characterization and cytotoxicity studies, J. Drug Deliv. Sci. Technol. 32 (2016) 1–9, https://doi.org/10.1016/j.jddst.2016.01.004.
[54] A. Rampino, M. Borgogna, P. Blasi, B. Bellich, A. Cesàro, Chitosan nanoparticles: preparation, size evolution and stability, Int. J. Pharm. 455 (1-2) (2013) 219–228, https://doi.org/10.1016/j.ijpharm.2013.07.034.
[55] S.A. Papadimitriou, D.S. Achilias, D.N. Bikiaris, Chitosan-g-PEG nanoparticles ionically crosslinked with poly(glutamic acid) and tripolyphosphate as protein delivery systems, Int. J. Pharm. 430 (1-2) (2012) 318–327, https://doi.org/10.1016/j.ijpharm.2012.04.004.
[56] J. Antoniou, F. Liu, H. Majeed, J. Qi, W. Yokoyama, F. Zhong, Physicochemical and morphological properties of size-controlled chitosan–tripolyphosphate nanoparticles, Colloids Surf, A Physicochem. Eng. Asp. 465 (2015) 137–146, https://doi.org/10.1016/j.colsurfa.2014.10.040.
[57] E.P. Cipolatti, A. Valério, G. Nicoletti, E. Theilacker, P.H.H. Araújo, C. Sayer, J.L. Ninow, D. de Oliveira, Immobilization of Candida antarctica lipase B on PEGylated poly(urea-urethane) nanoparticles by step miniemulsion polymerization, J. Mol. Catal., B Enzym. 109 (2014) 116–121, https://doi.org/10.1016/j.molcatb.2014.08.017.
[58] W. Al-Azzam, E.A. Pastrana, Y. Ferrer, Q. Huang, R. Schweitzer-Stenner, K. Griebenow, Structure of poly(Ethylene glycol)-Modified horseradish peroxidase in organic solvents: infrared amide I spectral changes upon protein dehydration are largely caused by protein structural changes and not by water removal per Se, Biophys. J. 83 (6) (2002) 3637–3651, https://doi.org/10.1016/s0006-3495(02)75364-2.
[59] G.-J. Zhou, G. Wang, J.-J. Xu, H.-Y. Chen, Reagentless chemiluminescence biosensor for determination of hydrogen peroxide based on the immobilization of horseradish peroxidase on biocompatible chitosan membrane, Sens. Actuators B Chem. 81 (2-3) (2002) 334–339, https://doi.org/10.1016/s0925-4005(01)00978-9.
[60] S. Shah, A. Pal, V.K. Kaushik, S. Devi, Preparation and characterization of venlafaxine hydrochloride-loaded chitosan nanoparticles and in vitro release of drug, J. Appl. Polym. Sci. 112 (5) (2009) 2876–2887, https://doi.org/10.1002/app.29807.
[61] J.-B. Qu, H.-H. Shao, G.-L. Jing, F. Huang, PEG-chitosan-coated iron oxide nanoparticles with high saturated magnetization as carriers of 10-hydroxycamptothecin: preparation, characterization and cytotoxicity studies, Colloids Surf. B Biointerfaces 102 (2013) 37–44, https://doi.org/10.1016/j.colsurfb.2012.08.004.
[62] M. Monier, D.M. Ayad, Y. Wei, A.A. Sarhan, Immobilization of horseradish peroxidase on modified chitosan beads, Int. J. Biol. Macromol. 46 (3) (2010) 324–330, https://doi.org/10.1016/j.ijbiomac.2009.12.018.
[63] D. Kulig, A. Zimoch-Korzycka, A. Jarmoluk, K. Marycz, Study on alginate–Chitosan complex formed with different polymers ratio, Polymers. 8 (5) (2016) 167, https://doi.org/10.3390/polym8050167.
[64] M.A. Hassan, A.M. Omer, E. Abbas, W.M.A. Baset, T.M. Tamer, Preparation, physicochemical characterization and antimicrobial activities of novel two phenolic chitosan Schiff base derivatives, Sci. Rep. 8 (1) (2018) 1–14, https://doi.org/10.1038/s41598-018-29650-w.
[65] A.A. Tagaç, Ö Sarp, K. Yurdakoç, Controlled release of vitamin C from chitosan nanoparticles, Hacettepe J. Biol. & Chem. 46 (1) (2018) 69–77, https://doi.org/10.15671/HJBC.2018.221.
[66] L.H. Gaabour, Spectroscopic and thermal analysis of polyacrylamide/chitosan (PAM/CS) blend loaded by gold nanoparticles, Results Phys. 7 (2017) 2153–2158, https://doi.org/10.1016/j.rinp.2017.06.027.
[67] J.A. Torres, F.G.E. Nogueira, M.C. Silva, J.H. Lopes, T.S. Tavares, T.C. Ramalho, A.D. Corrêa, Novel eco-friendly biocatalyst: soybean peroxidase immobilized onto activated carbon obtained from agricultural waste, RSC Adv. 7 (27) (2017) 16460–16466, https://doi.org/10.1039/c7ra01309d.
[68] N.P. Katuwavila, A.D.L.C. Perera, S.R. Samarakoon, P. Soysa, V. Karunaratne, G.A.J. Amaratunga, D.N. Karunaratne, Chitosan-alginate nanoparticle system efficiently delivers doxorubicin to MCF-7 cells, J. Nanomater. 2016 (2016) 1–12, https://doi.org/10.1155/2016/3178904.
[69] L.A. Kanis, F.C. Viel, J.S. Crespo, J.R. Bertolino, A.T. Pires, V. Soldi, Study of poly (ethylene oxide)/Carbopol blends through thermal analysis and infrared spectroscopy, Polymer 41 (9) (2000) 3303–3309, https://doi.org/10.1016/s0032-3861(99)00520-0.
[70] V. Sok, A. Fragoso, Preparation and characterization of alkaline phosphatase, horseradish peroxidase, and glucose oxidase conjugates with carboxylated carbon nano-onions, Prep. Biochem. Biotechnol. 48 (2) (2018) 136–143, https://doi.org/10.1080/10826068.2017.1405025.
[71] A.M. Elwerfalli, A. Al-Kinani, R.G. Alany, A. ElShaer, Nano-engineering chitosan particles to sustain the release of promethazine from orodispersables, Carbohydr. Polym. 131 (2015) 447–461, https://doi.org/10.1016/j.carbpol.2015.05.064.
[72] Z. Sobhani, S.M. Samani, H. Montaseri, E. Khezri, Nanoparticles of chitosan loaded ciprofloxacin: fabrication and antimicrobial activity, Adv. Pharm. Bull. 7 (3) (2017) 427–432, https://doi.org/10.15171/apb.2017.051.
[73] F. Bande, S.S. Arshad, M.H. Bejo, S.A. Kamba, A.R. Omar, Synthesis and characterization of chitosan-saponin nanoparticle for application in plasmid DNA delivery, J. Nanomater. 2015 (2015) 1–8, https://doi.org/10.1155/2015/371529.
[74] O. Borges, G. Borchard, J.C. Verhoef, A. de Sousa, H.E. Junginger, Preparation of coated nanoparticles for a new mucosal vaccine delivery system, Int. J. Pharm. 299 (1-2) (2005) 155–166, https://doi.org/10.1016/j.ijpharm.2005.04.037.
[75] E. Rostami, S. Kashanian, M. Askari, The effect of ultrasound wave on levothyroxine release from chitosan nanoparticles, Adv. Mater. Res. 829 (2013) 284–288, https://doi.org/10.4028/www.scientific.net/amr.829.
[76] M. Agarwal, M.K. Agarwal, N. Shrivastav, S. Pandey, R. Das, P. Gaur, Preparation of chitosan nanoparticles and their in-vitro characterization, Int. J. Life. Sci. Scienti. Res. 4 (2) (2018) 1713–1720, https://doi.org/10.21276/ijlssr.2018.4.2.17.
[77] A.V.A. Mariadoss, R. Vinayagam, V. Senthilkumar, P. Manickam, M. Kadarkarai, B. Xu, K.M. Gothandam, V.S. Kotakadi, E. David, Phloretin loaded chitosan nanoparticles augments the pH-dependent mitochondrial-mediated intrinsic apoptosis in human oral cancer cells, Int, J. Biol. Macromol. 130 (2019) 997–1008, https://doi.org/10.1016/j.ijbiomac.2019.03.031.
[78] S. Khoee, Y. Bagheri, A. Hashemi, Composition controlled synthesis of PCL–PEG Janus nanoparticles: magnetite nanoparticles prepared from one-pot photo-click reaction, Nanoscale. 7 (9) (2015) 4134–4148, https://doi.org/10.1039/c4nr06590e.
[79] A. Dwevedi, Basics of Enzyme Immobilization, Enzyme Immobilization, (2016), pp. 21–44, https://doi.org/10.1007/978-3-319-41418-8_2.

[80] D. Spasojević, M. Prokopijević, O. Prodanović, M.G. Pirtea, K. Radotić, R. Prodanović, Immobilization of chemically modified horseradish peroxidase within activated alginate beads, Hem. Ind. 68 (1) (2014) 117–122, https://doi.org/10.2298/HEMIND121122036S.

[81] N. Gupta, A. Shrivastava, R.K. Sharma, Silica nanoparticles coencapsulating gadolinium oxide and horseradish peroxidase for imaging and therapeutic applications, Int. J. Nanomedicine 7 (2012) 5491–5500, https://doi.org/10.2147/ijn.s33295.

[82] S.A. Mohamed, A.L. Al-Malki, T.A. Kumosani, R.M. El-Shishtawy, Horseradish peroxidase and chitosan: activation, immobilization and comparative results, Int. J. Biol. Macromol. 60 (2013) 295–300, https://doi.org/10.1016/j.ijbiomac.2013.06.003.

[83] B. Yu, H. Cheng, W. Zhuang, C.J. Zhu, J. Wu, H. Niu, D. Liu, Y. Chen, H. Ying, Stability and repeatability improvement of horseradish peroxidase by immobilization on amino-functionalized bacterial cellulose, Process Biochem. 79 (2019) 40–48, https://doi.org/10.1016/j.procbio.2018.12.024.

[84] Y. Liu, M. Wang, J. Li, Z. Li, P. He, H. Liu, J. Li, Highly active horseradish peroxidase immobilized in 1-butyl-3-methylimidazolium tetrafluoroborate room-temperature ionic liquid based sol–gel host materials, Chem. Commun. (13) (2005) 1778–1780, https://doi.org/10.1039/b417680d.

[85] K. Rani, N. Chauhan, J. Narang, U. Jain, S. Sharma, A cost effective immobilization of horseradish peroxidase nanoparticles on to easy-to-prepare activated plasticized polyvinyl-chloride vial and its application, J. Nanomed. Res. 2 (1) (2015) 1–5, https://doi.org/10.15406/jnmr.2015.02.00017.

[86] Y.-R. Chiu, W.-J. Ho, J.-S. Chao, C.-J. Yuan, Enzyme-encapsulated silica nanoparticle for cancer chemotherapy, J. Nanomed. Res. 14 (4) (2012) 1–10, https://doi.org/10.1007/s11051-012-0829-1.